# Hydrodynamic Studies of Adsorbed Diblock Copolymers in Porous Membranes

**Richard M. Webber, John L. Anderson,* and Myung S. Jhon**

*Department of Chemical Engineering, Carnegie Mellon University, Pittsburgh, Pennsylvania 15213.* *Received April 5, 1989; Revised Manuscript Received August 21, 1989*

ABSTRACT: Extension and surface coverage of adsorbed poly(2-vinylpyridine)/polystyrene (PVP/PS) diblock copolymers were studied by measuring their effect on convective transport in the pores of well-characterized mica membranes. When PVP/PS is adsorbed to a mica membrane from toluene, the PVP block anchors the diblock to the surface and the PS block imitates a terminally attached chain extending from the pore wall. The hydrodynamic thickness of the polymer layer in toluene was measured, and using a Debye–Brinkman model for the hydrodynamic interaction of the polymer segments with the fluid, it was concluded that the hydrodynamic thickness is a good measure of the polymer layer extension. This conclusion was further supported by agreement between the hydrodynamic thickness in toluene and the chain extension estimated from published force–distance measurements on the same diblock samples and by a constant hydrodynamic thickness over a range of shear rates ($10^3$–$10^4$ $s^{-1}$). The polymer layer was collapsed by replacing toluene with the nonsolvent heptane, and the hydrodynamic thickness measurements in heptane were used to estimate the surface coverage. Reversibility of the extension of the polymer layer to changes in solvent quality, from toluene to heptane to toluene, was observed.

## Introduction

Studies of polymers adsorbed to interfaces generally focus on two basic issues. The first involves the equilibrium relationship between the amount of polymer adsorbed and the concentration of the polymer dissolved in the adjoining solution.[1,2] The second issue, the configuration or ensemble-averaged segment density of the adsorbed polymer as a function of distance from the interface,[3-6] must be addressed in order to model the thermodynamics of the adsorption process. Investigation of the details of these two issues is of central importance to the many current applications of adsorbed polymers. For instance, in colloidal dispersions, stability is often determined as much by chain extension as by the amount of polymer adsorbed.[7] In cases where polymers are adsorbed to microporous membranes, membrane permeability and selectivity are strongly dependent on the conformation of the polymer.[8]

The unique properties of diblock copolymers, relative to the more commonly studied adsorbed homopolymers, are apparent when the diblock is designed such that each block is compatible with different solvents. The lyophobic block (insoluble or only marginally soluble in the chosen solvent) adsorbs to the surface, producing a flattened bulk-type conformation described as a "wetted" layer.[2] The lyophilic block (well solvated by the solvent) retains the more diffuse-type segment density associated with a polymer molecule in a good solvent and extends into solution away from the point of attachment.[3-6,9] The solvated chains expand such that osmotic forces balance the entropic restoring forces.[1-4,10] Figure 1a is a schematic of the adsorbed diblock copolymer layer for the solvent conditions described above. When adsorbed to a solid surface, amphiphilic diblock copolymers imitate terminally attached (grafted) chains and thus are expected to produce a very different segment density profile than that of adsorbed homopolymers.

Theoretical models attempting to describe the extension and segment density profile of terminally attached polymers have been proposed in the past. Fleer et al.,[5] de Gennes,[11] and Ploehn and Russel[12] review theories for the configuration of terminally attached polymer chains. At present, the models can be grouped into general categories: scaling theory,[3,4] mean field theory,[6] and self-consistent field calculations.[13] The simplicity and availability of these theories, and thus the potential for fundamentally understanding adsorbed polymer systems, motivate the experimental investigation of terminally attached polymers and the use of diblock copolymers to approximate this type of system.

Three basic experimental methods have been used to probe the configuration and extension of adsorbed polymers: spectroscopic techniques (ellipsometry, evanescent wave-induced fluorescence, and neutron scattering),[14-17] direct measurement of forces between surfaces with adsorbed polymers,[9,18,19] and transport measurements.[8,20-22] In this paper we are concerned with the last of these methods, particularly, retardation of viscous flow by adsorbed polymer.

The basic principle of hydrodynamic transport experiments is that the polymer segments represent Stokeslets (points of friction) for the fluid as it flows relative to the solid boundary because the segments move on average with the solid surface to which they are attached. Varoqui and Dejardin[23] described the essential features of the hydrodynamic effect for flow through porous membranes, while Anderson and Kim[24] generalized and extended the hydrodynamic description to colloidal particles. When the mean extension of the polymer is small relative to the radius of curvature of the solid boundary, the effect of the polymer on *all* laminar flows of solvent near the boundary can be represented by one parameter, the hydrodynamic thickness $L_H$, which depends only on the segment density profile for a given adsorbed polymer.[25]

In this paper we present the results of experiments designed to study hydrodynamic effects of adsorbed diblock polymers on pressure-driven flow of liquids through capillary-like pores in thin well-characterized membranes. The membrane pores act as a support for the adsorbed diblock copolymers. Since transport processes through the *bare* mica membrane are well understood, it is a straightforward matter to study the net effect of adsorbed polymer. The diblock copolymer we have employed in

* To whom correspondence should be addressed.

0024-9297/90/2223-1026$02.50/0 

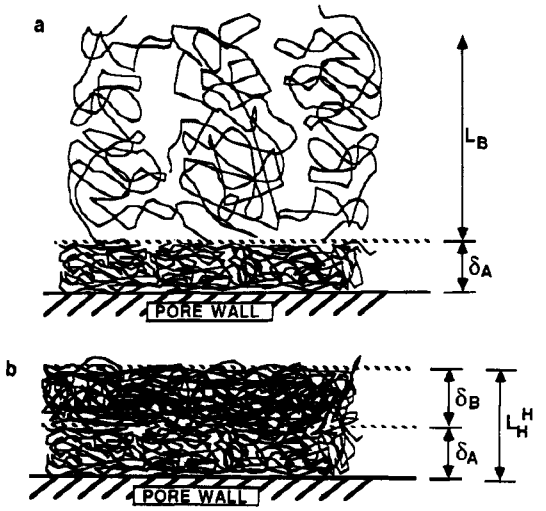


**Figure 1.** a. Schematic of PVP/PS adsorbed to pore wall surface in toluene. The PVP block forms a bulk layer of thickness $\delta_A$. The solvated PS chains imitate terminally attached chains and are anchored to the interface by the adsorbed PVP block. $L_B$ is some characteristic length scale that describes the physical thickness of the PS brush. b. Schematic of PVP/PS adsorbed to pore wall surface in heptane. The nonsolvated PS chains have collapsed onto the PVP layer to form a second bulk-density layer of thickness $\delta_B$. The overall thickness of the PVP and PS layers is the measured hydrodynamic thickness in heptane, $L_H^H = \delta_A + \delta_B$.

our studies is poly(2-vinylpyridine)/polystyrene (PVP/PS); our samples are the same as those used by Hadzioannou and co-workers[9,18,26] whose data indicate that PVP forms an anchor by adsorbing from toluene to a mica surface, with the PS chain extending into solution as illustrated in Figure 1.

The hydrodynamic experiments were performed with three liquids chosen for solvent quality with respect to the blocks of PVP/PS: toluene which is a good solvent for PS and a nonsolvent for PVP, *n*-heptane which is a nonsolvent for both PVP and PS, and methanol which is a nonsolvent for PS and a solvent for PVP. Methanol and heptane are miscible with toluene. The values of $L_H$ measured in heptane ($L_H^H$) are used to determine the amount of polymer adsorbed per area of pore wall. Simple models for the configuration of the adsorbed polymer and for liquid flow of solvent through the polymer chains are used to relate the measured hydrodynamic thickness in toluene ($L_H^T$) to the extension of the solubilized PS block.

## Experimental Section

The experiments consisted of applying a known pressure difference across a porous membrane while measuring the flow rate of polymer-free liquid. A schematic of the apparatus is shown in Figure 2. A constant flow rate was provided by a syringe pump; the pressure drop across the membrane was measured with a pressure transducer, and the liquid flow rate was determined by periodically weighing samples of the liquid passing through the membrane. The hydrodynamic permeability, defined as the ratio of the liquid flow rate to the applied pressure difference, was determined before and after adsorption of the polymer. The equivalent hydrodynamic thickness, $L_H$, is *defined* as the thickness of an impermeable layer that accounts for the reduction in membrane permeability due to the adsorbed polymer.

The membranes were made from thin sheets of muscovite mica, approximately 7 μm thick, by a track-etch technique.[27] With track-etched membranes, pores are created by etching the tracks created by collimated fission fragments from a Californium 252 source with a hydrofluoric acid solution. The number of pores ($n$) is controlled by the exposure time of the membrane to the fission source, while the pore radius is determined by the etching time, temperature, and concentration of the aqueous hydrofluoric acid bath. The pores are uniform in size and perpendicular to the membrane surface. The *uniformity* of pore size is an important feature of these membranes because a significant pore-size distribution would lead to ambiguous results for the hydrodynamic thickness of the polymer layer due to biased flow through the larger pores. The pore cross-sectional area fraction for the irradiated part of the membranes was approximately 1%; therefore, the total number of single pores, as modelled by a binomial pore-size distribution,[27] was greater than 96%. The pore length ($l$) equaled the membrane thickness, since the pores were perpendicular to the membrane face; the thickness was determined from the known dimensions and weight of the membrane.

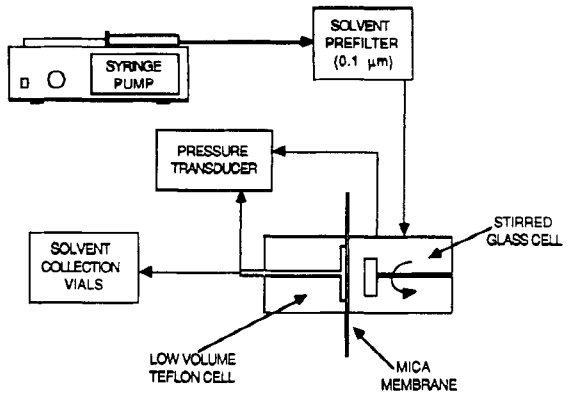


**Figure 2.** Schematic diagram of the flow apparatus. The liquid is filtered before passing through the mica membrane.

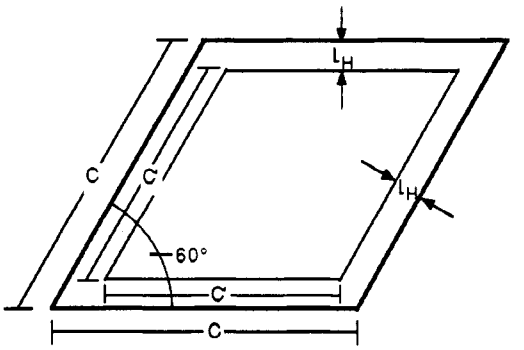


**Figure 3.** Illustration of the rhomboidal pore geometry of mica membranes, where $R_0$ is the radius of a circle of the same cross-sectional area as a 60° rhomboidal pore with sides of length $c$.

The pore cross section, illustrated in Figure 3, is a 60° rhombus. We define the pore radius to be the radius of a circle of equivalent area. The pore radius of a *bare* membrane ($R_0$) was determined before polymer was adsorbed by measuring the flow rate ($Q_0$) of toluene or heptane as a function of the pressure difference ($\Delta P$) across the membrane. The membrane permeability, $k_{H_0}$, is defined as

$$k_{H_0} \equiv \frac{\mu Q_0}{\Delta P} = [0.68]\left[\frac{n\pi R_0^4}{8l}\right]\left[1 + \frac{3\pi R_0}{8l}\right]^{-1} \quad (1)$$

where $\mu$ is the solvent viscosity. The second term (in brackets) is the Hagen–Poiseuille equation, which describes flow through circular channels of infinite $l/R_0$, while the third term is a correction for converging/diverging flow streamlines at the pore ends.[28] The factor 0.68 corrects for the shape of the pore; the pore is modeled as an ellipse of axis ratio 2.55, which has the same perimeter-to-area ratio as a 60° rhombus.[29] Error estimates for the independent determination of $n$ and $l$ are ±5% and ±1% respectively. Each membrane was calibrated (pore radius of a *bare* membrane determined) at least twice. From eq 1 the uncertainty in $R_0$ is computed to be ±2%.

The PVP/PS diblock copolymers were synthesized anionically by Hadziioannou et al.;[9] the molecular weights are listed

**Table I**
**Properties of the PVP/PS Diblock Copolymers[a]**

| polym designatn | $M_w$ PVP | $M_w$ PS | r, Å toluene | r, Å θ conditns | $M_A/M_B$ |
|---|---|---|---|---|---|
| 60/60 | 60 000 | 60 000 | 218 | 175 | 1.00 |
| 55/186 | 54 500 | 185 500 | 420 | 308 | 0.29 |
| 28/95 | 28 000 | 95 000 | 285 | 220 | 0.29 |
| 5/45 | 5 000 | 45 000 | 185 | 152 | 0.11 |
| PS100 | | 100 000 | 293 | 226 | |

[a] The diblocks (and homopolymer) are designated by the molecular weight of each block in thousands. $M_w$ is the weight-average molecular weight of the respective block.[9] $r$ is the rms end-to-end distance of a free PS chain of the same $M_w$ as in the diblock copolymer ($r$ was estimated by multiplying the radius of gyration of the free PS chain in toluene[41] by $\sqrt{6}$).

in Table I. (Note that the diblock labeling scheme is slightly different here than that used in other papers,[9,18,26] although they are the same diblock samples.) Polydispersity indices for all the diblocks were less than 1.2.[9,18] Adsorption of the polymer was achieved by contacting the membrane in situ with a 70 μg/mL solution of PVP/PS in toluene at room temperature (typically 22 °C) for a specific time. This contact occurred in the glass cell of the pressure drop/flow rate apparatus (Figure 2). The cell was filled with polymer solution, and the polymer was allowed to diffuse into the membrane pores while the cell was stirred. The polymer solution was then removed, and the membrane was rinsed with pure toluene. The polymer-coated membrane was allowed to equilibrate in toluene. In this manner, the PVP/PS solution could also be recontacted with the membrane to continue the adsorption process.

Polystyrene was purchased from Pressure Chemical Co. and had a polydispersity index of less than 1.1; the molecular weight was 100 000. A 4.0 mg/mL solution of polystyrene in toluene was prepared and contacted with membrane 90 for 48 h, which is the same time used to adsorb the PVP/PS copolymers.

The liquids were purchased from Fisher Scientific: Spectranalyzed toluene and HPLC grade *n*-heptane and methanol. The liquids were filtered for removal of particulates with 0.1-μm pore-size Nucleopore filters prior to contact with a membrane. Preparation of the polymer solution was done with filtered toluene. The polymer solutions were also filtered before contact with the membrane. In addition, the experimental apparatus upstream to the membrane was rinsed thoroughly with filtered toluene before assembling the flow cell with the membrane. Fouling of any membrane (i.e., a decrease in hydraulic permeability over time) was not observed.

Figure 4 shows sample data. Experiments were performed over a wide range of applied pressure to check for nonlinear flows that could result from flow-induced conformational changes of the adsorbed polymer of fouling of the membrane. Good proportionality was observed between $\mu Q$ and $\Delta P$ with or without polymer adsorbed to the membrane, even at the highest shear rates ($\dot{\gamma}$ is defined as $Q/n\pi R_0^3$). By plotting $\mu Q$, rather than $Q$, we can directly compare data taken at different temperatures and with different fluids. The temperature, typically 22 °C, varied by less than ±0.5 °C throughout an experiment.

Figure 4 also illustrates the general experimental approach to investigating the diblock copolymer layer. After membrane calibration, adsorption of the polymer, and equilibration of the polymer layer in toluene, the hydrodynamic experiments were run with toluene. The toluene was then replaced by heptane and the hydrodynamic experiments repeated (the same procedure was followed when methanol was the flowing liquid). Membranes were allowed 1–2 h of contact with a new liquid for removal of the previous liquid and equilibration of the adsorbed diblock-copolymer/membrane system before the hydrodynamic experiments were performed. Permeability experiments were usually run several times to check for reproducibility; if the hydrodynamic permeability ($k_H$) was constant over several experiments for a particular solvent condition, it was concluded that this was enough time for the adsorbed polymer to reach a steady conformational state in the new solvent. In all adsorbed diblock-copolymer/membrane systems, we found reversibility in the permeability in going from toluene → heptane → toluene. In no case did we ever detect desorption of the polymer, which would have been indicated by an increase in $k_H$ for a given solvent over time, throughout the duration of a full series of experiments with a particular membrane (the longest series ran for over a month).

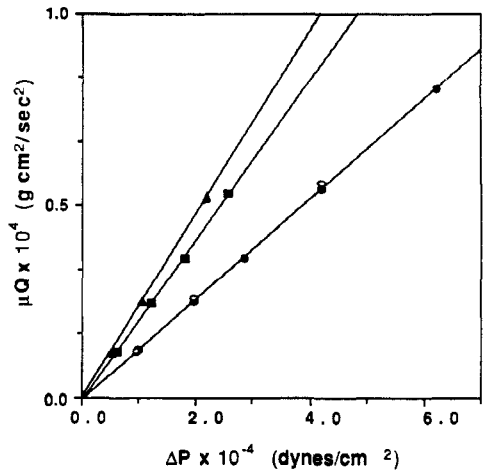


**Figure 4.** Sample data for $\mu Q$ versus $\Delta P$ plot ($R_0$ = 2550 Å). Symbol nomenclature: (▲) membrane pore size calibration (no polymer); (●) experimental run in toluene after the adsorption of the 60/60 PVP/PS diblock; (■) after collapse of PS block in the nonsolvent heptane; (○) after re-expansion of the PS block in toluene. Best-fit straight lines are drawn through the data points; the slope gives the permeability, $k_H$.

Drying of the diblock-copolymer/membrane system was accomplished by draining toluene from the flow cell, allowing the residual toluene to evaporate from the low volume side at room temperature, and then placing the cell and membrane into an oven at 42 °C for 10–12 h. The total drying time was greater than 24 h. The membranes were judged to be dry when air could be forced through with no detectable pressure drop. The diblock-copolymer/membrane system was rewet with heptane by slowly forcing heptane through the membrane to fill the low-volume side of the flow cell. The membrane was continuously flushed in this manner for several hours before hydrodynamic experiments were conducted.

## Results

The results of our hydrodynamic experiments are presented as the equivalent hydrodynamic thickness of the adsorbed polymer, which is calculated from

$$L_H = [1.21]^{-1}R_0\left[1 - \left[\frac{k_H}{k_{H_0}}\right]^{1/4}\right] \quad (2)$$

where $R_0$ is computed from eq 1. The subscript 0 means that the experiment was run before polymer was adsorbed. The prefactor $[1.21]^{-1}$ corrects for the rhomboidal geometry of the pores in the mica membrane, as illustrated in Figure 3. $L_H$ represents the thickness of a totally impermeable layer that must be applied to the pore walls to account for the reduction in the hydrodynamic permeability of the membrane caused by the polymer; it is not necessarily equal to the actual thickness of the polymer layer.

Table II summarizes our measurements of the hydrodynamic thickness in both toluene ($L_H^T$) and heptane ($L_H^H$) for the four diblock samples. *Reversibility* of the hydrodynamic thickness to changes in the solvent quality for the PS chains in the sequence toluene → heptane → toluene was observed, as shown in Figures 4 and 5a; that is, we always recovered the same $L_H^T$ even after contacting the membrane with heptane for several days. $L_H^T$ values listed in Table II are average values for the hydrodynamic thickness before and after exposure to hep-

**Table II**
**Hydrodynamic Thickness of Polymer Layer versus Pore Radius of the Mica Membrane, $R_0$[a]**

| polymer [membrane] | $R_0$, Å | $L_H^T$,[b] Å toluene | $L_H^H$, Å heptane | $r/R_0$ |
|---|---|---|---|---|
| 60/60 [54] | 4360 | 300 ± 30 | 80 ± 30 | 0.05 |
| [61] | 2550 | 280 ± 10 | 80 ± 10 | 0.09 |
| [77] | 1820 | 300 ± 20 | 20 ± 20[c] | 0.12 |
| [47] | 1200 | 360 ± 10 | 80 ± 10 | 0.18 |
| [40] | 590 | 150 ± 10[d] | 10 ± 10 | 0.37 |
| 55/186 [87] | 5030 | 560 ± 130 (± 27) | 10 ± 260 (±50) | 0.08 |
| [84] | 4300 | 510 ± 10 | −40 ± 10 | 0.10 |
| 28/95 [58] | 3240 | 540 ± 10 | 90 ± 10 | 0.09 |
| 5/45 [88] | 4820 | 340 ± 100 (± 63) | 90 ± 110 (±20) | 0.04 |
| [71] | 3390 | 380 ± 30 | 90 ± 30 | 0.06 |

[a] Except for membrane 40, values of $L_H$ are for conditions where adsorption of the polymer had reached equilibrium. The numbers in brackets are membrane designations. $L_H^T$ and $L_H^H$ are the hydrodynamic thicknesses in toluene and heptane, respectively, $r$ is the rms end-to-end distance of the PS block in toluene (see Table I). The average *maximum* error in the membrane pore radius is ±2%. *Maximum* error estimates are given:; error values in parentheses were determined from the standard deviation of $L_H$ measurements. [b] Average of values measured before and after contact with heptane. [c] Only one $L_H^H$ experiment was performed. [d] Adsorption equilibrium may not have been achieved.

tane. Estimates of the *maximum* error in $L_H$ are listed in Table II and were determined from a *worst*-case error analysis of eq 2. For those situations where the error analysis resulted in exceptionally large estimates, the standard deviation of the $L_H$ values is listed to indicate experimental reproducibility (in each of these cases at least five separate permeability experiments were performed to determine a mean $L_H$). As discussed below, the values of $L_H$ presented in Table II are for conditions where the polymer appeared to be adsorbed to equilibrium coverage.

The kinetics of adsorption were studied by contacting the membrane with the polymer solution for a certain time, determining the membrane permeabilities for the toluene → heptane → toluene sequence described in the Experimental Section, and then re-exposing the membrane to the polymer solution. Sample data are plotted in Figure 6 to qualitatively demonstrate the kinetics of PVP/PS adsorption. The pore wall was assumed to be at equilibrium with the PVP/PS solution when $k_H$ for toluene and heptane no longer decreased with further exposure of the membrane to the polymer solution. In general, the total exposure of the membrane to the polymer solution in these experiments was greater than 48 h, which seemed to be more than enough time to achieve equilibrium adsorption.

Three comments about the adsorption of these diblock polymers to mica membranes are worth mentioning. First, the relatively slow progression of the diblock-copolymer/membrane system to the equilibrium state *cannot* be attributed to hindered diffusion of polymer through the pores. The time scale for diffusion of the polymer through the length of the pore is small, ≈10 s, allowing for hindrance effects caused by the finite polymer-to-pore size ratio,[30] compared to the contact time of ≈$10^4$ s needed to reach equilibrium adsorption. Tassin et al.[26] also observed apparent kinetic limitations to adsorption at flat surfaces with three of the same polymers used in our study. Second, other data from our experiments similar to that plotted in Figure 6 reveal that the two diblocks with the shorter PVP chains, 5/45 and 28/95, reach equilibrium adsorption significantly faster than the 60/60 and 55/186 diblocks. Finally, because the PVP/PS solutions were filtered before contact with the mica membranes, it is possible that these solutions were at concentrations below the critical micelle concentration (cmc),

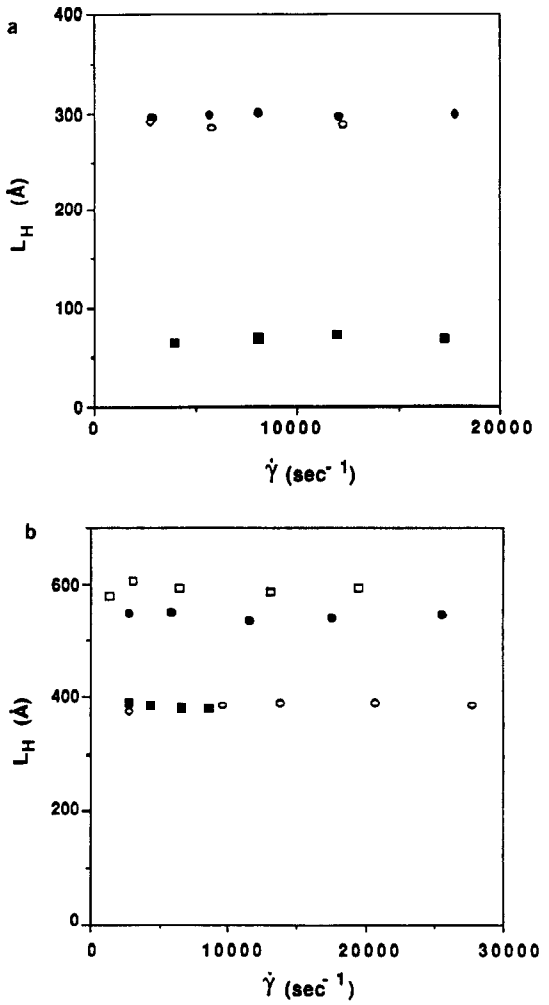


**Figure 5.** a. Hydrodynamic thickness ($L_H$) as a function of shear rate ($\dot{\gamma} = Q/n\pi R_0^3$) for the 60/60 PVP/PS ($R_0$ = 2550 Å). Symbol nomenclature: (●) initial measurements with toluene ($L_H^T$); (■) after change to heptane ($L_H^H$); and (○) after re-expansion in toluene ($L_H^T$). b. $L_H^T$ as a function of shear rate ($\dot{\gamma}$) for the PVP/PS diblock copolymers. Symbol nomenclature: (●) 28/95 PVP/PS ($R_0$ = 3240 Å); (○) 5/45 PVP/PS ($R_0$ = 3390 Å); (■) 60/60 PVP/PS ($R_0$ = 1200 Å); (□) 55/186 PVP/PS ($R_0$ = 5030 Å).

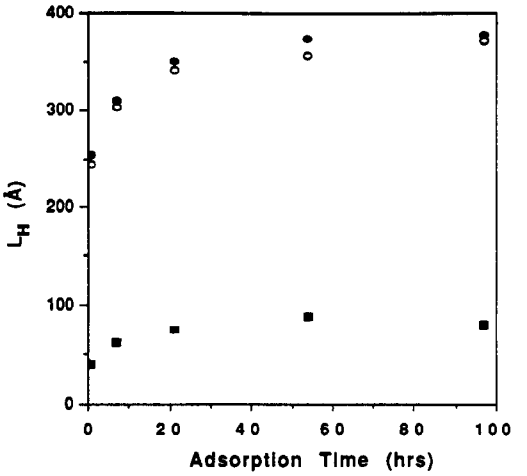


**Figure 6.** $L_H$ as a function of adsorption time for 60/60 PVP/PS ($R_0$ = 1200 Å). Symbol nomenclature: (●) $L_H^T$ in toluene after exposure of the membrane to polymer solution; (■) $L_H^H$ after collapse in heptane; (○) $L_H^T$ after re-expansion in toluene.

Table III
Hydrodynamic Thickness (in Å) of the Polymer Layer for the Sequence of Experimental Conditions Designed To Investigate *Negative* Values of $L_H^H$ [a]

| polymer [membrane] | $R_0$, Å | from Table III | | | after exposure to MeOH | | | | after drying | | |
|---|---|---|---|---|---|---|---|---|---|---|---|
| | | $L_H^T$ | $L_H^H$ | $L_H^T$ | $L_H^M$ | $L_H^T$ | $L_H^H$ | $L_H^T$ | $L_H^H$ | $L_H^T$ | $L_H^H$ |
| 5/45 [88] | 4820 | 330 | 90 | 350 | 200 | 330 | 110 | 330 | 60 (± 34) | 350 | 70 |
| 55/186 [87] | 5030 | 540 | 10 | 570 | 200 | 610 | 80 | 560 | 70 (± 13) | 530 | -10 |
| [84] | 4300 | 510 | -40 | 510 | 200 | 660 | 120 | 630 | | | |
| PS100[b] [90] | 1630 | 110 | -60 | 100 | -70 | 30 | -80 | 20 | | | |

[a] $L_H^M$ is the hydrodynamic thicknesses in methanol. After exposure of the polymer layer to MeOH, the polymer layer was contacted with toluene and then heptane. The membrane was dried and then re-exposed to heptane and toluene, and finally, $L_H^H$ was measured. Error estimates are consistent with those listed in Table II, and error values in parentheses were determined from the standard deviation of $L_H$ measurements. [b] An estimate of the maximum error in $L_H$ is ±30 Å. The polystyrene homopolymer (PS100) was adsorbed from a concentrated toluene solution (4.0 mg/mL).

which is about 65 μg/mL for the 5/45 and 60/60 diblocks.[31] Tassin et al.[26] reported that concentrations of this polymer above and below the cmc give essentially the same equilibrium surface coverage, while Munch and Gast[32] reported that the equilibrium surface coverage for a PEO/PS diblock depends on the concentration, with polymer solutions below the cmc giving higher equilibrium surface coverages.

Table II indicates that there is a pore size effect for the 60/60 diblock when $r/R_0 \geq 0.18$, where $r$ is the root-mean-square end-to-end distance of the corresponding isolated PS chain in toluene solution. While this result is perhaps not surprising, little can be made of it in a quantitative sense because of the difficulty in understanding effects of the nonuniform curvature (i.e., corners) of rhomboidal pores and the difficulty in interpreting $L_H$ when it is a large fraction of the pore radius. In general, the data indicate that $L_H$ increases as $R_0$ decreases, as observed in studies with homopolymers.[8,22] With the smallest pores ($R_0$ = 590 Å), we found that equilibrium adsorption was not achieved after 90 h of contact with a solution of the 60/60 diblock. For membranes with large pores ($r/R_0 \leq 0.1$) there was no appreciable pore-size effect on the value of $L_H$.

Our experiments with toluene and heptane showed no dependence of $L_H$ on shear rate. Figure 5 illustrates that $L_H$ is essentially constant over the range of shear rates ($\dot{\gamma} \approx 10^3$–$10^4$ $s^{-1}$) attainable in our experiments. The absence of shear-rate effects implies the polymer layer had a fairly sharp outer edge, although it is possible that some highly extended chains were already flattened at high shear rates of order $10^3$ $s^{-1}$.

Puzzling results were obtained for the 55/186 diblock (see membranes 84 and 87 in Table II). Upon changing the liquid from toluene to heptane (by the procedure outlined in the previous section) the membrane permeability *increased* over that of the membrane *before* the adsorption of the 55/186 diblock, resulting in a *negative* $L_H$. Negative values of $L_H^H$ were observed for six other membranes with the 55/186 diblock adsorbed (data not presented here). Negative values of $L_H^H$ persisted even after extended contact (several days) of the membrane with heptane, yet we observed *reversibility* to changes in solvent and were able to recover the original positive values of $L_H^T$ after recontact with toluene. Therefore, a simple argument such as defects (cracks) in the membrane cannot explain these data. Negative values of $L_H^H$ were not observed with diblocks other than the 55/186.

A series of experiments was designed to investigate the negative values of $L_H^H$. Membrane 88, with the 5/45 diblock adsorbed, acted as a control and was exposed to the identical experimental history as membrane 87 with 55/186 adsorbed. The experimental history of solvent changes is toluene → heptane → toluene → methanol → toluene → heptane → toluene → membrane dried → rewet with heptane → toluene → heptane. After each change of solvent, the hydrodynamic thickness of the polymer layer was measured; the results are given in Table III. After the drying step, the flow experiments with heptane gave *positive* values of $L_H^H$. We believe that the membrane was completely rewet after drying because when the liquid was changed from heptane to toluene, the measured value of $L_H^T$ was the same as the value before drying. Most interesting is the fact that $L_H^H$ was again *negative* or small for membrane 87 after the toluene reexposure step (see last column of Table III).

In addition to the experiments with PVP/PS described above, a homopolymer of styrene (PS100) was studied to see whether or not PS would adsorb to mica from concentrated solutions and also to aid in understanding the negative values of $L_H^H$ obtained with the 55/186 diblock copolymer. The experimental history of membrane 90 is given in Table III. The adsorbed PS100 exhibited *negative* values of $L_H$ in heptane as well as *reversibility* to the solvent changes between toluene and heptane. Furthermore, the adsorbed PS100 also exhibited *negative* values of $L_H$ with exposure to methanol, but after exposure of the membrane to methanol, the original hydrodynamic thickness in toluene ($L_H^T$) was *not* recovered.

Adsorption of PS100 from *dilute* solutions (≈70 μg/mL) ranging from good to poor in solvent quality (by increasing the percent volume of heptane with respect to toluene) was also attempted. The measured values of $L_H^T$ were so small as to be experimentally insignificant. These results imply that at the *dilute* concentrations of our diblock polymers, there was negligible adsorption of the PS block.

## Analysis and Discussion

**Physical Model of Polymer Layer.** The two extreme conformations of the polymer layer that we envision are shown in Figure 1. Because toluene is a nonsolvent for PVP, the PVP block adsorbs to the mica pore wall to anchor the PS chain. (This was confirmed by the observation that PS100 did not adsorb from toluene at 70 μg/mL.) The density of the PVP layer is assumed to equal the bulk-solid value when the liquid phase is either toluene or heptane, since both liquids are nonsolvents for PVP.[33] We assume a uniform layer of PVP on the pore wall; however, this assumption cannot be checked directly by our experiments. The PS chains are in an expanded state when toluene is the liquid but collapse into a "dense" state when heptane replaces the toluene. Because heptane is a nonsolvent for PS and does not swell this polymer,[34] we estimate that the density of the PS layer in heptane equals the bulk-solid value.

As noted in the previous section, the negative values of $L_H^H$ observed with the 55/186 diblocks cannot be explained by defects (e.g., holes) in the membranes. A negative value for $L_H$ arises when the measured membrane permeability is greater with the polymer adsorbed than for the bare membrane. A possible explanation for this behavior is that the viscosity of the liquid in the pores is overestimated; for instance, if toluene is trapped in the collapsed PS layer when the fluid is changed from toluene to heptane, toluene would be expected to mix with heptane so that the fluid in the pore is no longer pure heptane. It is well-known that mixtures of two simple liquids, such as toluene and methanol, can exhibit lower viscosities than either pure liquid.[35] If the viscosity of the fluid within certain regions of the pores is less than the pure liquid value assumed in eq 2, then a negative $L_H$ might be computed. From Table III (membrane 90) it is noted that PS100 exhibits a negative value for $L_H$ in both heptane and methanol. The adsorbed diblocks would not be expected to exhibit negative values for $L_H$ in methanol since methanol is a good solvent for PVP[31,33] and would be expected to swell the PVP layer; this is confirmed by the data presented in Table III.

Membranes 87 and 88 (see Table III) were dried and then rewet with heptane according to the procedure detailed in the Experimental Section. Both membranes exhibited *positive* values for $L_H$ in heptane after drying. The 5/45 and 55/186 diblock layers were re-expanded in toluene. The final two columns in Table III indicate that *after* the drying procedure and then re-exposure of the membrane to toluene, the diblock layers returned to the state that was observed for the measurements listed in Table II. Negative values of $L_H^H$ were once again observed for the 55/186 polymer after collapse from toluene to heptane. These results suggest that a mixed-solvent effect in going from toluene to heptane could have been responsible for the negative values of $L_H^H$ observed with the 55/186 diblock; however, we do not understand at present why the other diblocks were not similarly affected.

**Surface Coverage.** Our strategy is to use the hydrodynamic measurements with heptane for a given diblock-copolymer/membrane system to compute the amount of polymer adsorbed per area of pore wall ($\Gamma$) and the thickness of PVP layer ($\delta_A$). Assuming both blocks are "dense" phases in heptane, the hydrodynamic thickness equals the sum of the two condensed layers

$$L_H^H = [\delta_A + \delta_B] \tag{3}$$

where the subscripts A and B denote PVP and PS, respectively. With this interpretation, a material balance on the condensed layers gives

$$\Gamma = L_H^H[M_A + M_B]\left[\frac{M_A}{\rho_A} + \frac{M_B}{\rho_B}\right]^{-1} \tag{4}$$

where $M_i$ and $\rho_i$ are the molecular weight and density for the i block. The number of PS chains per area of pore wall ($\sigma$) is given by

$$\sigma = \frac{\Gamma N_0}{[M_A + M_B]} \tag{5}$$

where $N_0$ is Avogadro's number. Finally, the thickness of the PVP layer, which is assumed to be the same for heptane and toluene, is

$$\delta_A = \frac{\Gamma}{\rho_A}\left[1 + \frac{M_B}{M_A}\right]^{-1} \tag{6}$$

**Table IV**
**Adsorption Parameters Determined from the $L_H^H$ Values[a]**

| polymer | $R_0$, Å | $\Gamma$, mg/m$^2$ | $10^2a^2\sigma$ | $\delta_A$, Å | $\sigma N_A^{2/3}$ | $\sigma N_A^{0.5}N_B^{0.3}$ |
|---|---|---|---|---|---|---|
| 60/60 | 4360 | 8.5 ± 3.1 | 1.0 ± 0.4 | 40 | $3.0 \times 10^{-2}$ | $6.9 \times 10^{-2}$ |
| | 2550 | 8.6 ± 0.7 | 1.0 ± 0.1 | 40 | $3.0 \times 10^{-2}$ | $7.0 \times 10^{-2}$ |
| 55/186 | 5030 | 7.1 ± 1.0[b] | 0.4 ± 0.1 | 10 | $1.2 \times 10^{-2}$ | $3.8 \times 10^{-2}$ |
| 28/95 | 3240 | 9.2 ± 0.9 | 1.0 ± 0.1 | 20 | $1.9 \times 10^{-2}$ | $5.7 \times 10^{-2}$ |
| 5/45 | 4820 | 9.1 ± 2.0 | 2.5 ± 0.6 | 10 | $1.5 \times 10^{-2}$ | $4.7 \times 10^{-2}$ |
| | 4820 | 6.0 ± 3.0[b] | 1.7 ± 1.0 | 10 | $1.0 \times 10^{-2}$ | $3.1 \times 10^{-2}$ |
| | 3390 | 10.0 ± 3.8 | 2.8 ± 1.1 | 10 | $1.6 \times 10^{-2}$ | $5.2 \times 10^{-2}$ |

[a] $\Gamma$ is the surface coverage. The PS chain surface density, $\sigma$, has been made dimensionless by $a^2$, where $a$ is the size of a PS segment (4.8 Å). $\delta_A$ is the thickness of the PVP bulk-type layer, where $L_H^H = \delta_A + \delta_B$. In these calculations the density of each block layer is assumed to be the bulk solid density: $\rho_A$[42] = 1.17 g/cm$^3$ and $\rho_B$ = 1.05 g/cm$^3$. Errors are based on the maximum error estimates listed in Table II. [b] Surface coverages calculated from $L_H^H$ measurements after drying listed in Table III.

Values of the above parameters obtained from the $L_H^H$ data in Table II are shown in Table IV. The surface coverage for the 55/186 diblock was calculated from the value of $L_H^H$ measured after drying the membrane (listed in Table III). The surface coverage of the 5/45 diblock (membrane 88) that was calculated from the value of $L_H^H$ after drying is also listed in Table IV. $\sigma$ has been nondimensionalized by $a^2$, where $a$ is the segment size estimated from the Flory expression[36] describing a PS chain in toluene (≈4.8 Å). $a^2\sigma$ is a measure of the area fraction of the pore wall occupied by terminal attachments sites for PS chains. The surface coverages ($\Gamma$) presented in Table IV are consistent with those measured for the equilibrium adsorption of the 5/45, 60/60, and 55/186 diblock samples on a silver surface;[26] however, our values of $\Gamma$ are higher by factors of 2–5 than those determined for adsorption of poly(2-vinylpyridine)/polyisoprene diblock polymer from toluene to the *basal* plane (surface) of mica.[37] A higher adsorption to the pore wall of mica is to be expected since this etched surface has a higher affinity for adsorbing amphiphilic molecules.[38]

Patel et al.[10] and Munch and Gast[1] have formulated predictions for the relationship between $\sigma$ and the block molecular weights of the polymer. Patel et al. suggested that the adsorption density is determined by the size of the nonsolvated block ($N_i$ is the number of monomers in the i block), which scales as $\sim N_A^{1/3}$; therefore, the surface density scales as $\sigma \sim N_A^{-2/3}$. Munch and Gast used a mean field theoretical approach to determine the total free energy of a system of adsorbed diblocks in equilibrium with a diblock solution; numerical analysis of their model suggested that diblock adsorption scales as $\sigma \sim N_A^{-0.5}N_B^{-0.3}$ when the A block is small relative to the B block ($M_A/M_B < 0.1$). In Table IV we list our experimentally determined surface coverages normalized by the two scaling relationships. Given the error limits on $\sigma$, we cannot reach a conclusion about which exponent on $N_A$ is correct. The data do suggest that there is a dependence on $N_B$, which is in qualitative agreement with the Munch and Gast theory.

**Hydrodynamic Model and Polymer Layer Extension.** Because toluene is a nonsolvent for PVP, we assume that the PVP layer is condensed, as shown in Figure 1a, and essentially unchanged from its configuration in heptane; therefore, the effective hydrodynamic thickness of the PS chains is $L^* = L_H^T - \delta_A$. From the $\delta_A$ values listed in Table IV, it can be seen that almost the entire

hydrodynamic thickness of the adsorbed diblock layer in toluene is provided by the solvated PS chains.

$L_H$ is a measure of the hydrodynamic resistance between the adsorbed polymer and the liquid as it flows through the pores. The total friction between the adsorbed polymer and the fluid is a measure of the physical extension of the polymer molecules away from the adsorption interface. The local polymer friction effect, operating at the segment length scale, can be modelled by using a Brinkman permeability coefficient ($\kappa^2$), such that under low Reynolds number flow conditions the fluid velocity v is described by the Debye–Brinkman equation[21,23,24] and conservation of fluid mass

$$\mu\nabla^2\mathbf{v} - \nabla p - \mu\kappa^2\mathbf{v} = 0 \tag{7a}$$

$$\nabla\cdot\mathbf{v} = 0 \tag{7b}$$

where $\mu$ is the viscosity coefficient of the liquid. $\kappa^2$ depends on the local polymer segment density $\rho(y)$, where $y$ is the distance from the pore wall; if this relationship is known and a model for $\rho(y)$ is postulated, then eq 7 can be solved and compared with the experimental value of $L_H$ to determine a "true" length scale for extension of the adsorbed polymer layer.

Varoqui and Dejardin[23] solved the Debye–Brinkman equation for polymer adsorbed to cylindrical pores, assuming an exponentially decaying profile for $\rho(y)$ and free draining of fluid through the segments. A more general hydrodynamic formulation was developed by Anderson and Kim[24] for polymer adsorbed to spherical particles. Their model for the hydrodynamic thickness can be generalized to any laminar flow, including flow through porous media, when $L_H$ is small relative to the length scale of the flow (here, the pore radius).[25] To determine $L_H$ from the properties of the adsorbed polymer, the following equation must be solved for the function $G(y)$

$$\frac{d^2G}{dy^2} - \kappa^2 G = 0 \tag{8a}$$

where $\kappa^2$ is a function of $y$ and $G$ is proportional to the retardation of the fluid velocity caused by the polymer. The boundary conditions are given by

$$y = 0 \qquad G = 0 \tag{8b}$$

$$y \to \infty \qquad \frac{dG}{dy} \to -1 \tag{8c}$$

$L_H$ is given by

$$L_H = \lim_{y\to\infty}[G + y] \tag{8d}$$

This result can be used with measured values of $L_H$ and an experimentally measured functionality of $\kappa^2$ with $\rho(y)$ to deduce properties of the polymer layer.

As discussed previously, a number of authors[3,4,6,13] have proposed theoretical models to describe the segment density profile of a polymer layer of terminally grafted polymer chains. In general, two different surface coverage regimes have been proposed to categorize polymer layers in pure fluids: a regime of noninteracting chains (low $a^2\sigma$)[4,11] and a regime of overlapping chains (large $a^2\sigma$).[3,4] Scaling arguments imply that the transition between these regimes is determined by size of the terminally attached chain were it in free solution; therefore, the overlapping chain regime is defined by $a^2\sigma \gg N_B^{-6/5}$. The scaling arguments of Alexander[3] and de Gennes[4] and some of the self-consistent field lattice calculations of Cosgrove et al.[13] qualitatively describe the polymer segment density profile as constant over a distance $L_B$ from the solid surface.

The measured values of $a^2\sigma$ listed in Table IV indicate that our polymer layers are in the overlapping chain regime. We have chosen a hypothetical step-function segment density profile as an approximate description of the polymer layer when toluene was the liquid

$$\rho_B(y) = \begin{cases} \rho_0 & 0 < y < L_B \\ 0 & y > L_B \end{cases} \tag{9}$$

where $\rho_B(y)$ is the local sensity density within the B layer (see Figure 1a). For the PVP/PS diblock with toluene as the liquid, the pore wall ($y = 0$) is defined as the outer edge of layer A (see Figure 1a); therefore, the $L_H$ of eq 8d is $L^*$, the hydrodynamic thickness of the solvated PS chains. The two parameters that describe the segment density profile, $\rho_0$ and $L_B$, are determined from the experimental values $\Gamma_B$ and L* and the hydrodynamic model. $\Gamma_B$ is the surface coverage due to the presence of the PS chains, so $\Gamma_B$ is given by

$$\Gamma_B = \Gamma\left[\frac{M_B}{M_A + M_B}\right]$$

where values of $\Gamma$ are listed in Table IV. With eq 9 we have

$$\Gamma_B = \int_0^\infty \rho_B(y)\, dy = \rho_0 \tag{10}$$

To solve eq 8 and thus determine $L_B$, a relationship between the Brinkman permeability coefficient $\kappa^2$ and $\rho_B(y)$ is required. Roots et al.[39] reported experimental values for the sedimentation coefficient for overlapping polystyrene chains over the concentration range 0.001–0.13 g/cm$^3$. The sedimentation coefficient ($s$) is related to the permeability coefficient through[39,40]

$$\kappa^{-2} = \frac{\mu s}{c(1 - \nu/\nu_s)} \tag{11}$$

where $\mu$ is the pure solvent viscosity, $\nu$ and $\nu_s$ are the partial specific volumes of the solute and fluid, respectively, and $c$ is the segment concentration. In the high concentration range (0.06–0.13 g/cm$^3$) the data are fit well by the following empirical relation

$$\kappa^2 = H\rho_B{}^m \tag{12}$$

with $H = 9.96 \times 10^{15}$ cm$^{-2}$(cm$^3$/g)$^m$ and $m = 2.04$.

The general solution to eq 8d using eqs 8a–c, 9, 10, and 12 can be expressed in terms of a dimensionless parameter, $\beta$

$$L^* = L_B F(\beta) \tag{13}$$

where

$$\beta = HL_B{}^2\rho_0{}^m = HL_B{}^{2-m}\Gamma_B{}^m \tag{14}$$

The function $F$ depends on the segment density profile. For the model step-function segment density profile given by eq 9, eq 8 is solved analytically to obtain

$$F(\beta) = 1 - \frac{\tanh\sqrt{\beta}}{\sqrt{\beta}} \tag{15}$$

$L_B$ is found by substituting the experimental values for $\Gamma_B$ and $L^*$ into eqs 13–15; the results are listed in Table V.

The step function model for the segment density profile of the PS chains shows that $L_B \approx L^*$; that is, $L_H$ is essentially a direct measure of the extension of the PS block in toluene. This is true because $\beta \gg 1$, which means

Table V
Effective Hydrodynamic Thickness ($L^*$) and Calculated Thickness ($L_B$) of the PS Chains in Toluene[a]

| polymer | $R_0$, Å | $L^*$, Å | $L_B$, Å | $L^*/r$ | $L^*\sigma^{-1/3}N_B^{-1}$ | $L^*N_B^{-0.7}N_A^{-0.17}$ |
|---|---|---|---|---|---|---|
| 60/60 | 4360 | 260 | 270 | 1.19 | 4.6 | 1.0 |
| | 2550 | 240 | 250 | 1.10 | 5.5 | 1.0 |
| 55/186 | 5030 | 550 | 560 | 1.31 | 5.5 | 1.0 |
| 28/95 | 3240 | 520 | 530 | 1.86 | 7.4 | 1.7 |
| 5/45 | 4820 | 330 | 330 | 1.78 | 7.8[b] | 2.4 |
| | 3390 | 370 | 370 | 2.00 | 8.0 | 2.7 |

[a] $L_B$ is the thickness of the polymer layer calculated from the hydrodynamic model with the assumption of a constant segment density within the polymer layer. [b] Calculated from average of values for $\sigma$.

Table VI
Comparison of the Hydrodynamic Thickness in Toluene, $L_H^T$, and the Thickness, $\delta^{sf}$, Estimated from the Force vs Distance Measurements of Tirrell et al.[18] on the Same Diblock Copolymer Samples in Toluene

| polymer | $L_H^T$, Å | $\delta^{sf}$, Å |
|---|---|---|
| 60/60 | 290[a] | 250 |
| 55/186[b] | 540[a] | 600–1100[c] |
| 28/95 | 540 | |
| 5/45[b] | 360[a] | 300 |
| 60/90 | | 375 |

[a] $L_H^T$ values are presented as an average of $L_H^T$ values from membranes 54 and 61 for the 60/60 diblock, membranes 88 and 71 for the 5/45 diblock, and membranes 84 and 87 for the 55/186 diblock. [b] Tirrell et al.[18] and Tassin et al.[26] have labeled the 5/45 and 55/186 diblocks as 5/60 and 60/150, respectively. [c] Estimation of $\delta^{sf}$ for the 55/186 diblock is difficult because of the shape of the force vs distance profile; a range of possible values for $\delta^{sf}$ is presented.

that there was no significant flow through any part of the PS layer. The absence of shear-rate effects on $L_H^T$ is consistent with a dense "brush" structure for the solvated PS layer, at least in the range of shear rates studied here. Use of a more realistic segment profile, such as that predicted by the self-consistent field lattice calculations of Cosgrove et al.,[13] would probably not significantly increase the values of $L_B$ relative to $L^*$. The purpose of our simple model is to show that the hydrodynamic thickness is, in fact, a characteristic *physical* length scale of the solvated portion of adsorbed diblock copolymers in the overlap surface coverage regime.

Table VI shows a comparison between our hydrodynamic thicknesses ($L_H^T$) and thicknesses for the same diblock polymers in toluene estimated from the surface-force apparatus ($\delta^{sf}$) of Tirrell et al.[18] $\delta^{sf}$ was estimated from the force vs distance data by associating the diblock layer thickness with the separation distance between the mica surfaces at a force $F/R \approx 50$ $\mu$N/m. Agreement of the hydrodynamic thickness with $\delta^{sf}$ is good, a fact which serves to strengthen our conclusions reached about the equivalence between $L^*$ and $L_B$. This agreement might at first seem inconsistent with the fact that our values of $\sigma$ are higher than those measured for the surface-force apparatus experiments;[37] however, the dependence on the surface coverage is predicted to be weak ($L_B \sim \sigma^{1/3}$), as discussed below.

A convenient way to evaluate the extension of the PS chains of the diblock copolymer layer is to associate the measured hydrodynamic thickness with the equilibrium size of the chain were it unattached in free solution. In Table V we compare $L^*$ to the root-mean-square end-to-end distance ($r$) of the PS chain were it freely dissolved in toluene.[41] Table V shows that as $a^2\sigma$ increases the relative extension of the PS chain increases; the chains are stretched compared to their equilibrium conformations in free solution.

de Gennes[4] suggested that the thickness of a layer of terminally attached chains scales as $L_B \sim aN_B\sigma^{1/3}$. Munch and Gast[1] considered adsorption of diblock copolymers from solution and derived the relationship $L_B \sim N_B^{0.7}N_A^{0.17}$. In the final two columns of Table V we present the measured thicknesses of the PS chains ($L^*$) normalized by each of these scaling relationships (for de Gennes' expression we used experimental values of $\sigma$ in the normalization). The data are perhaps too limited in range and accuracy to judge the quantitative correctness of either model, but the similarity of $L_H^T$ measurements for the 55/186 and 28/95 diblock copolymers implies that the polymer layer thickness depends on the molecular weight of both blocks.

## Summary

The experiments indicate that the hydrodynamic thickness of diblock copolymers that are relatively monodisperse, where one block preferentially adsorbs to the liquid/solid interface, is approximately equal to the actual extension of the polymer from the interface at sufficiently high surface coverages, an equivalence that does not hold for adsorbed homopolymers. The layer thicknesses we measured are in good agreement with the values deduced for the same diblock polymers adsorbed to mica in a surface–force apparatus. Further evidence of a dense "brush" is given by the fact that there was no shear thinning of the polymer layer over the shear-rate range of $10^3$–$10^4$ $s^{-1}$.

Another important observation is that the solvated portion of the polymer, the PS block in our case, could be *reversibly* collapsed and expanded by changing the solvent from toluene to heptane to toluene. We collapsed the PS block 5–9-fold (the overall polymer layer by 4–8-fold) and re-expanded it by changing the solvent. Furthermore, re-expansion of the polymer layer was achieved in toluene even after drying liquid from the pores. These reversible conformational changes of the expandable block might prove useful in developing membranes with "tunable" properties.

## Nomenclature

| | |
|---|---|
| $a$ | polymer segment size (Å) |
| $k_{H_0}$ | membrane permeability without adsorbed polymer $\mu Q_0/\Delta P$ ($cm^3$) |
| $k_H$ | membrane permeability with polymer adsorbed $\mu Q/\Delta P$ ($cm^3$) |
| $L_B$ | physical thickness of solvated B chains of adsorbed diblock polymer (Å) |
| $L_H^T$ | hydrodynamic thickness of adsorbed polymer in toluene (Å) |
| $L_H^H$ | hydrodynamic thickness of adsorbed polymer in heptane (Å) |
| $L_H^M$ | hydrodynamic thickness of adsorbed polymer in methanol (Å) |
| $L^*$ | hydrodynamic thickness of solvated PS chains, $L_H^T - \delta_A$ (Å) |
| $l$ | pore length (cm) |
| $M_i$ | weight-average molecular weight of i block of diblock copolymer (g/mol) |
| $N_i$ | number of monomer segments in i block of diblock copolymer |
| $N_0$ | Avogadro's number (molecules/mol) |
| $n$ | number of pores in a mica membrane |
| $Q$ | flow rate of liquid through membrane ($cm^3/s$) |
| $R_0$ | radius of pores in a bare mica membrane (Å) |

| | |
|---|---|
| $r$ | root-mean-square end-to-end distance of the corresponding PS chain of a diblock in toluene (unperturbed by adsorption) (Å) |
| $s$ | sedimentation coefficient (s) |
| $\mathbf{v}$ | fluid velocity (cm/s) |
| $y$ | distance from adsorbing surface (cm) |
| $\Gamma$ | surface coverage (mg/m$^2$) |
| $\dot{\gamma}$ | shear rate $Q/n\pi R_0^3$ (s$^{-1}$) |
| $\Delta P$ | pressure drop across the mica membrane (dyn/cm$^2$) |
| $\delta_i$ | thickness of collapsed i layer of adsorbed diblock polymer (nonsolvated state) (Å) |
| $\delta^{sf}$ | thickness of adsorbed PVP/PS measured by surface-force apparatus (in toluene) (Å) |
| $\kappa^2$ | Brinkman permeability coefficient (cm$^{-2}$) |
| $\mu$ | pure liquid viscosity (g/cm s) |
| $\nu$ | partial specific volume of solute (cm$^3$/g) |
| $\nu_s$ | partial specific volume of fluid (cm$^3$/g) |
| $\rho_i$ | density of collapsed i layer of adsorbed diblock polymer (bulk density) (g/cm$^3$) |
| $\sigma$ | number of apparent terminally attached chains per area (grafts/Å$^2$) |

## Subscripts i

| | |
|---|---|
| A | PVP block of diblock copolymer PVP/PS |
| B | PS block of diblock copolymer PVP/PS |

**Acknowledgment.** This work was supported by the National Science Foundation and the IBM Center for Thin Film Sciences at Carnegie Mellon University. We thank Drs. M. Tirrell and G. Hadziioannou for providing us with the diblock copolymers and for sharing their experimental results with us.

## References and Notes

(1) Munch, M. R.; Gast, A. P. *Macromolecules* **1988**, *21*, 1366.
(2) Marques, C.; Joanny, J. F.; Leibler, L. *Macromolecules* **1988**, *21*, 1051.
(3) Alexander, S. *J. Phys. (Les Ulis, Fr.)* **1977**, *38*, 983.
(4) de Gennes, P. G. *Macromolecules* **1980**, *13*, 1069.
(5) Fleer, G. J.; Scheutjens, J.; Cohen Stuart, M. A. *Colloids Surf.* **1988**, *31*, 1.
(6) Milner, S. T.; Witten, T. A.; Cates, M. E. *Macromolecules* **1988**, *21*, 2610.
(7) Napper, D. H. *Polymeric Stabilization of Colloidal Dispersions*; Academic: London, 1983.
(8) Kim, J. O.; Anderson, J. L. *J. Membrane Sci.* **1989**, *47*, 163.
(9) Hadziioannou, G.; Patel, S.; Granick, S.; Tirrell, M. *J. Am. Chem. Soc.* **1986**, *108*, 2869.
(10) Patel, S.; Tirrell, M.; Hadziioannou, G. *Colloids Surf.* **1988**, *31*, 157.
(11) de Gennes, P. G. *Adv. Colloid Interface Sci.* **1987**, *27*, 189.
(12) Ploehn, H. J.; Russel, W. B. *Adv. Chem. Eng.*, in press.
(13) Cosgrove, T.; Heath, T.; van Lent, B.; Leermakers, F.; Scheutjens, J. *Macromolecules* **1987**, *20*, 1692.
(14) Takahashi, A.; Kawaguchi, M.; Hirota, H.; Kato, T. *Macromolecules* **1980**, *13*, 884.
(15) Ausserre, D.; Hervet, H.; Rondelez, F. *Macromolecules* **1986**, *19*, 85.
(16) Cosgrove, T.; Heath, T. G.; Ryan, K.; van Lent, B. *Polym. Commun.* **1987**, *28*, 64.
(17) Cosgrove, T.; Crowley, T. L.; Vincent, B. In *Adsorption from Solution*; Rochester, C. H., Ottewill, R. H., Smith, A. L., Eds.; Academic: New York, 1983.
(18) Tirrell, M.; Patel, S.; Hadziioannou, G. *Proc. Natl. Acad. Sci. U.S.A.* **1987**, *84*, 4725.
(19) Taunton, H. J.; Toprakcioglu, C.; Fetters, L. J.; Klein, J. *Nature* **1988**, *332*, 712.
(20) Pefferkorn, E.; Dejardin, P.; Varoqui, R. *J. Colloid Interface Sci.* **1978**, *63*, 353.
(21) Cohen Stuart, M. A.; Waajen, F. H. W. H.; Cosgrove, T.; Vincent, B.; Crowley, T. *Macromolecules* **1984**, *17*, 1825.
(22) Idol, W. K.; Anderson, J. L. *J. Membr. Sci.* **1986**, *28*, 269.
(23) Varoqui, R.; Dejardin, P. *J. Chem. Phys.* **1977**, *66*, 4395.
(24) Anderson, J. L.; Kim, J. *J. Chem. Phys.* **1987**, *86*, 5163.
(25) Anderson, J. L.; McKenzie, P. F.; Webber, R. M., submitted for publication.
(26) Tassin, J. F.; Siemens, R. L.; Tang, W. T.; Hadziioannou, G.; Swalen, J. D.; Smith, B. A. *IBM Res. Rep.* **1988**, *RJ6252* 61649.
(27) Quinn, J. A.; Anderson, J. L.; Ho, W. S.; Petzny, W. J. *Biophys. J.* **1972**, *12*, 990.
(28) Happel, J.; Brenner, H. *Low Reynolds Number Hydrodynamics*; Nijhoff: Dordrecht, 1983.
(29) Munch, W. D.; Zestar, L. P.; Anderson, J. L. *J. Membr. Sci.* **1979**, *5*, 77.
(30) Kathawalla, I. A.; Anderson, J. L. *Ind. Chem. Eng. Res.* **1988**, *27*, 866.
(31) Tang, W. T. Ph.D. Thesis, Stanford University, 1987.
(32) Munch, M. R.; Gast, A. P. *Trans. Faraday Soc.*, in press.
(33) Selb, J.; Gallot, Y. *Polymer* **1979**, *20*, 1259.
(34) Errede, L. A.; Stoesz, J. D.; Sirvio, L. M. *J. Appl. Polym. Sci.* **1987**, *31*, 2721.
(35) Teitelbaum, B. Y.; Gortalova, T. A.; Ganelina, S. G. *J. Gen. Chem. USSR (Engl. Transl.)* **1950**, *20*, 1422.
(36) Flory, P. J. *Principles of Polymer Chemistry*; Cornell University Press: Ithaca, 1953.
(37) Watanabe, H.; Tirrell, M. *Polym. Prepr. (Am. Chem. Soc., Div. Polym. Chem.)* **1989**, *30*, 387.
(38) Petzny, W. J.; Quinn, J. A. *Science* **1969**, *168*, 751.
(39) Roots, J.; Nyström, B.; Sundelöf, L.-O.; Porsch, B. *Polymer* **1979**, *20*, 337.
(40) Mijnlieff, P. F.; Jaspers, W. J. M. *Trans. Faraday Soc.* **1971**, *67*, 1837.
(41) Varma, B. K.; Fujita, Y.; Takahashi, M.; Nose, T. *J. Polym. Sci.* **1984**, *22*, 1781.
(42) Arichi, S.; Matsuura, H.; Tanimoto, Y.; Murata, H. *Bull. Chem. Soc. Jpn.* **1966**, *39*, 434.

**Registry No.** (PVP)(PS) (block copolymer), 108614-86-4; muscovite mica, 1318-94-1.